doi: 10.29382/eqs-2020-0034-04

Multiple phases analysis of deep seismic sounding records in North China Craton*

Xiaoqing Zhang[1,2,✉] Jiyan Lin[1,2,3] Minghui Zhang[4] Zhi Liu[3] Baofeng Liu[3] Youshan Liu[1] Tao Xu[1,5] Zhiming Bai[1]

[1] *State Key Laboratory of Lithospheric Evolution*, *Institute of Geology and Geophysics*, *Chinese Academy of Sciences*, *Beijing* 100029, *China*
[2] *University of Chinese Academy of Sciences*, *Beijing* 100049, *China*
[3] *Geophysical Exploration Center*, *China Earthquake Administration*, *Zhengzhou* 450002, *China*
[4] *Institute of Information Engineering*, *Binzhou University*, *Binzhou*, *Shandong* 256600, *China*
[5] *CAS Center for Excellence in Tibetan Plateau Earth Sciences*, *Beijing* 100101, *China*

Abstract The North China Craton (NCC) is a key region to study the destruction of the ancient craton. Two groups of phases (denoted as "Pw1" and "Pw2"), which are parallel to the PmP phase reflected from the Moho discontinuity and the PLP phase reflected from the Lithosphere and Asthenosphere Boundary(LAB) respectively, are found on the record section of the Rongcheng-Xinzhou-Alxa long-range deep seismic sounding profile. The nature of the two phases is still unclear, although they are clearly observable and reverberant. In this paper, we use travel time inversion and amplitude forward modelling to fit the reflected and refracted phases in the lithosphere. The results show: (1) the Pw1 is a multiple reflected phase which is successively reflected by the crystalline basement, the surface, the Moho and then finally received on the surface; (2) the Pw2 phase is also a multiple reflected phase successively reflected by the crystalline basement, the surface, the LAB interface and then received on the surface. We conclude that the significant velocity difference between the thick sedimentary cover and the crystalline basement in the North China rifted basin may be the main reason for generating the multiple reflections. Furthermore, the two multiple reflections provide potent constraints on the lithospheric velocity model, and constitute seismological evidence for the lithospheric thinning in the eastern NCC.

Keywords: North China Craton; deep seismic sounding; multiple reflections; lithospheric structure

* **Received** 4 March 2020; **accepted in revised form** 25 March 2020; **published** 30 November 2020.

✉ **Corresponding author. e-mail**: zxq@mail.iggcas.ac.cn

1 Introduction

Cratons are an important geological unit on the Earth, and cover about 1/2 of the continent (Rudnick and Fountain, 1995). North China Craton (NCC) is one of the oldest cratons in the world, preserving continental rocks about 3.8 Ga (Liu et al., 1992). The NCC was originally formed by the amalgamation of the eastern and western blocks along the Central Orogenic Belt at ~1.8 Ga and remained relatively stable with a thick Archan lithosphere root until the early Mesozoic (Zhao et al., 2001, 2005). However, previous studies show that the structure, physical-chemical properties and stability of the NCC have been reworded, with the development of large-scale structural deformation and magmatic activity since the Mesozoic (Xu, 2001, 2004b; Lin et al., 2004; Wang et al., 2005; Zhang, 2005; Wu et al., 2005; Zheng et al., 2005, 2008, 2009, 2014, 2017; Chang et al., 2007; Chen et al., 2008, 2009, 2014; Chen, 2010; Zheng et al., 2015; Duan et al., 2016; Zhu et al., 2017). Therefore, the NCC is the best place to study the destruction of ancient cratons. In recent years, scholars in China and abroad have carried out intensive systematic studies on the destruction of the NCC, and further established the craton destruction theory. This theory holds that unsteady mantle flow induced by the west-dipping subduction of the paleo-West Pacific plate (the Izanagi plate) is the most important external control factor and driving force for the destruction of the NCC. What's more, it clarifies the universal law of global continental evolution that the cratonic destruction and continental accretion are generally caused by the interaction between the continent and ocean, and further to enrich and push the plate tectonics theory (Zhu and Zheng,

2009; Zhao et al., 2009, 2012; Zhu et al., 2011, 2012).

Since the 1950s, deep seismic sounding has been one of the important ways to understand the interior structure, dynamics of the earth as well as explore mineral resources (Zelt and Smith, 1992; Prodehl and Mooney, 2012; Jia et al., 2009; Zhang et al., 2011; Teng et al., 2013; Zhang et al., 2013; Xu et al., 2014a, 2014b, 2015; Zhang et al., 2015). Long deep seismic sounding profiles expose the deep structural of different blocks, which are important accurately understanding the physical properties of the lithosphere mantle (Roller and Jackson, 1966; Egorkin, 1998; Teng, 2003; Malinowski et al., 2009; Zhao et al., 2009; Jia et al., 2014; Tian et al., 2014; Wang et al., 2014; Liu et al., 2015; Duan et al., 2015, 2016). In 2009, a 1650 km long refraction/reflection profile (the Rongcheng-Xinzhou-Alxa profile) that extends E-W across the entire NCC has been finished supported by the National Science Foundation of China (NSFC) (Liu et al., 2015; Figure 1). The results reveal significant regional variation that the crustal and lithospheric thickness displays a general increase from SE to NW. Particularly, it presents an obvious uplift of the Moho and lithosphere interface beneath the North China rifted basin (Wang et al., 2014; Jia et al., 2014; Tian et al., 2014). Liu et al. (2015) obtained the P-wave velocity structure of the crust and mantle beneath the eastern section of this profile, and the results show that the Moho and the Lithosphere and Asthenosphere Boundary (LAB) below the basin are complex and may be a sharp transition layer, which may be related to the destruction of the NCC.

Furthermore, two phases with strong amplitudes have been identified after the PmP phase and PLP phase on the section from the east branch of the shot Sp5 of this profile. In this essay, we attempt to use the 2D ray-tracing method to discuss the causes and natures of the two phases, and to provide more seismic constraints for the lithospheric structure of the eastern NCC.

2 Multiple phase analysis

The Rongcheng-Xinzhou-Alxa profile that extends E-W across the entire NCC from west to east, whose length is up to 1 650 km and shots were fired at the 11 sites (1.2–11.0 tons of each shot). As shown in Figure 2, on the recording section with the reduced velocity of 8.0 km/s from the east branch of the shot Sp5, a series of phases with high signal to noise ratio are identified. A strongly reflected phase from the Moho (PmP) is clearly observed at the offsets between 80 km and 220 km. The mantle diving wave (Pn) with an apparent velocity of 8.0 km/s, which is observed at larger offsets (150–400 km) and arrive significantly earlier. A weak reflected phase from the LAB has been identified at the offsets range from approx 350 km to 550 km, which are separated by time gaps (1 s later in the reduced section) from the Pn arrivals. Phase identification was confirmed through the checking of reciprocal travel times, which has been proved especially useful in identifying the PmP and PLP phases. The P-wave velocity model of the whole lithosphere beneath this recording section are constructed (Liu et al., 2015).

However, two obvious seismic phases on this record sections have not been explained in detail. As shown in Figure 2, a continuously trackable phase is clearly observed behind the PmP phase at offsets between 100 km and 200 km, which is called Pw1 phases here. The Pw1 phase is approximately parallel to the PmP phase, and its relative reduced traveltime difference is about 2.4–2.9 s. Meanwhile, a reverberant phase is observed behind the PLP phase at offsets between 380–600 km, denoted Pw2

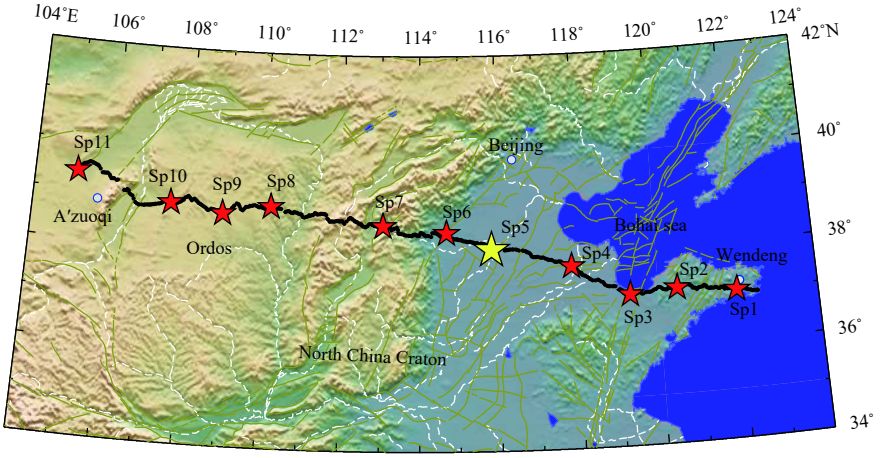

Figure 1 The location map of Rongcheng-Xinzhou-Alxa deep seismic sounding profile. The record section for shot Sp5, marked by a yellow star, is used in this paper (modified from Liu et al., 2015)

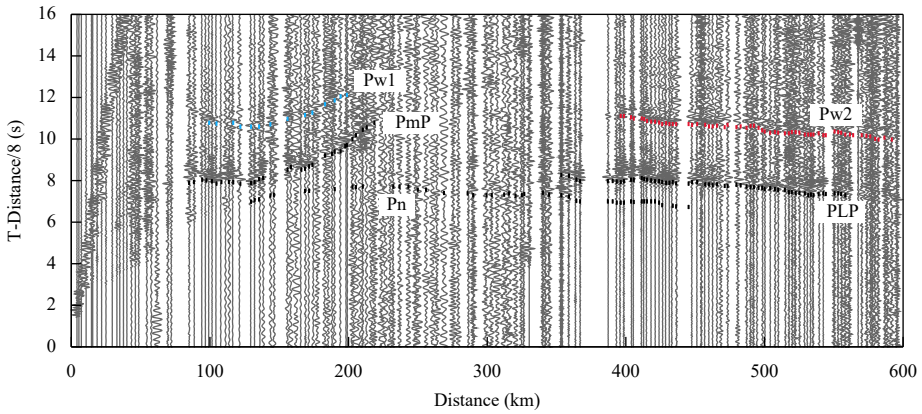

Figure 2 Identified phases on the record section from the east branch of shot Sp5 (modified from Liu et al., 2015)

phases here, which is approximately parallel to the PLP phases, and its relative reduced traveltime difference is about 2.7–3.2 s.

From the reduced recording section shown in Figure 2, it is apparent that the Pw1 and Pw2 phases are clearly identified indicating the picked travel times of two phase are reliable. It is worth noting that the Pw1 phase is approximately parallel to the PmP phase, and the slope of their traveltime-distance curve is approximately equal. What's more, the reduced traveltime difference of the two phases is not varying with the epicentre distance. The features between the Pw2 and PLP phase are the same. Taken together, the most possible scenario is that Pw1 and Pw2 are multiple waves of PmP and PLP respectively. In the following, the 2D ray-tracing method will be used to prove this hypothesis.

3 Forward modelling

3.1 Method

In this paper, travel times of all phases were picked using ZPlot, and interactive plotting and picking software package (Zelt and Smith, 1992). The accuracy of the picking is range from 50 ms to 200 ms. And the ray-tracing program RAYINVR (Zelt and Smith, 1992) was used for 2D forward modelling and inversion, which is based on the layered structure modelling, and invert the 2D velocity and interface structure simultaneously via damped least-squares inversion to minimize the travel time residuals. RAYINVR also can estimate the resolution, uncertainty, and non-uniqueness of model parameters to avoid over-fitting. Even though this method is invented for more than 30 years, it is still widely used in the interpretation of deep seismic sounding data (Xu et al., 2006, 2010, 2014).

Ray equation is solved by a numerical method in the RAYINVR forward modelling:

$$\frac{\partial x}{\partial t} = v\sin\theta,\ \frac{\partial z}{\partial t} = v\cos\theta,\ \frac{\partial \theta}{\partial t} = -\cos\theta\frac{\partial v}{\partial x} + \sin\theta\frac{\partial v}{\partial z}. \quad (1)$$

Damped least-square inversion is used to minimize the traveltime residuals:

$$\Delta \boldsymbol{m} = (\boldsymbol{A}^{\mathrm{T}}\boldsymbol{C}_{\boldsymbol{t}}{}^{-1}\boldsymbol{A} + d\boldsymbol{C}_{\boldsymbol{m}}{}^{-1})^{-1}\boldsymbol{A}^{\mathrm{T}}\boldsymbol{C}_{\boldsymbol{t}}{}^{-1}\Delta \boldsymbol{t}, \quad (2)$$

where $\Delta\boldsymbol{m}$ is the perturbation vector of the model parameter (velocity or interface depth); $\Delta\boldsymbol{t}$ is the traveltime residual vector; $\boldsymbol{A}$ is partial differential matrix of traveltime relative to model parameters; d is the global damping factor; $\boldsymbol{C_t}$ and $\boldsymbol{C_m}$ are the covariance matrix of the estimated data and model (Zelt and Smith, 1992).

3.2 Velocity structure of the crust and upper mantle

Liu (2015) has obtained 2D P-wave crustal and mantle velocity model beneath the Rongcheng-Xinzhou-Alxa profile. We simplified the model and establish a P-wave velocity model (Figure 3) beneath the North China rifted basin and Luxi uplift. This model has three layers: sedimentary cover, crystalline crust and lithospheric mantle. The thickness of sedimentary cover is 0.5 km to 4.8 km, with a P-wave velocity 2.0 km/s to 4.8 km/s; the crystalline crust has a thickness of 33.1–34.5 km, and the P wave velocity is 5.9–6.9 km/s. The thickness of lithosphere is 72.0–78.5 km, and its P-wave velocity in the lithospheric mantle is about 8.0–8.3 km/s.

3.3 Traveltime modelling

Based on the aforementioned velocity in section 3.2, we propose the following four assumptions of the Pw1 and Pw2 wave propagation path and then calculate travel times.

(1) Multiples between the ground and the Moho discontinuity: one scenario is that the Pw1 phase is multiples that propagate downward from the shot point, and then is

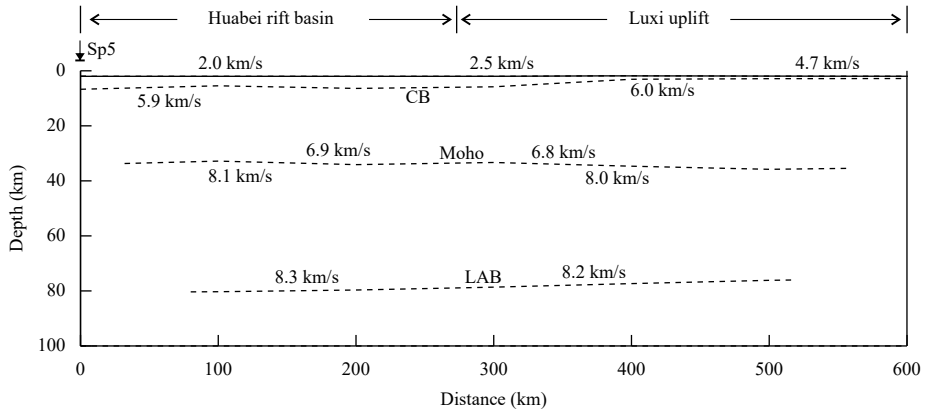

Figure 3 A simplified 2D P-wave velocity model of crust and upper mantle adapted from Liu et al. (2015). CB refers to crystalline basement, LAB refers to Lithosphere and Asthenosphere Boundary

successively reflected by the Moho discontinuity, the surface, the Moho discontinuity and received on the surface. The Pw2 phase is multiples that reflected back to the surface by the LAB interface after a reflection from the Moho and the surface (Figure 4a). The theoretical traveltimes of the two phases based on this assumption is shown in dashed line (a) in Figure 5. Both of them have a time delay of 2.0–3.0 s comparing with the travel times of the Pw1 and Pw2 phase. Therefore, this assumption does not hold.

(2) Multiples between the crystalline basement and Moho discontinuity: another hypothesis is the Pw1 phase is multiples that propagate downward from the shot point, and then successively reflected by the Moho discontinuity, the bottom of crystalline basement, the Moho discontinuity and then received on the surface. The Pw2 phase is multiples that reflected back to the surface by the LAB interface after a reflection from the Moho and the bottom of crystalline basement (Figure 4b). As shown in dashed line (b) in Figure 5, there is time gap (about 1.5 s to 3.5 s later) between the calculated traveltimes and the observed which indicate this assumption is false.

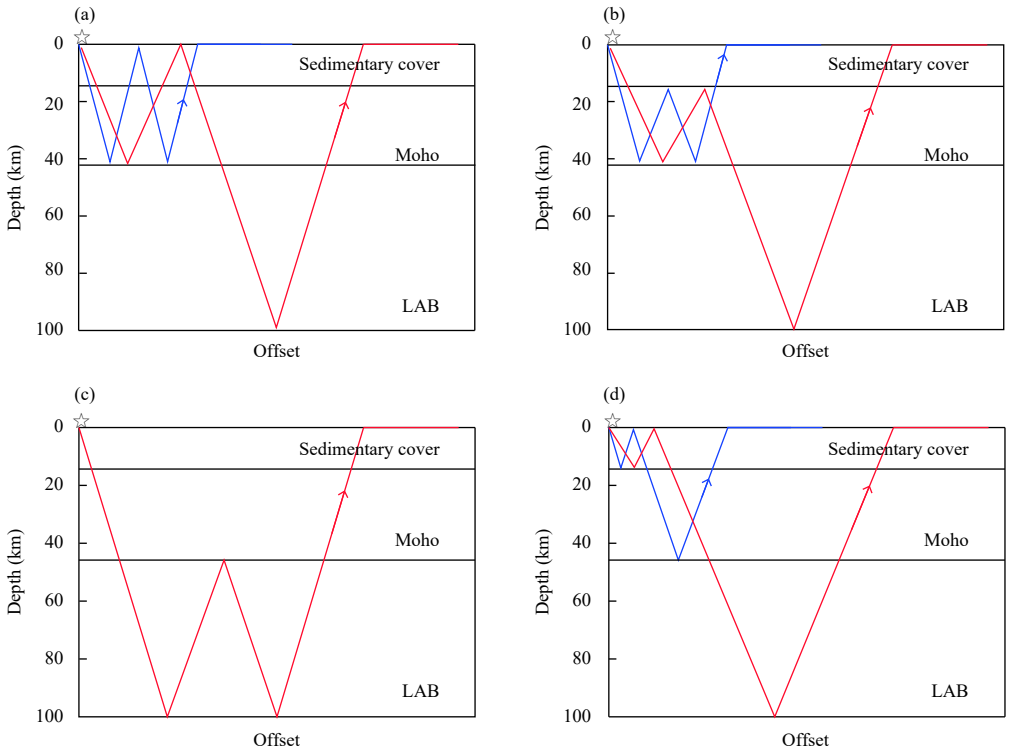

Figure 4 Simply diagram of possible multiple ray paths. The blue line indicates the ray path of Pw1 phase and the red line indicates the ray path of Pw2 pahse

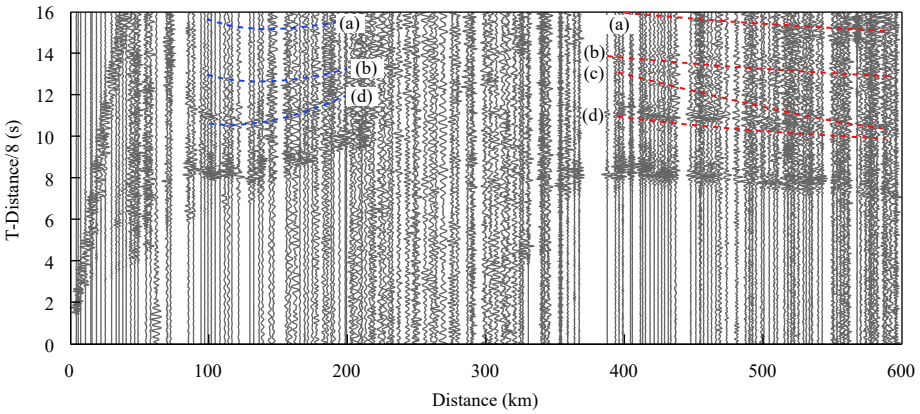

Figure 5 Comparison of synthetic traveltimes of Pw1 and Pw2 phases caculated for four different raypath shown in Figure 4. The blue dotted line and the red dotted line represent the calculated traveltimes of Pw1 phase and Pw2 phase, respectively

(3) Multiples between the Moho and LAB discontinuity: a possible scenario is the Pw2 phase propagate downward from the shot point and then successively reflected by the LAB discontinuity, the Moho discontinuity, the LAB discontinuity and finally received on the surface (Figure 4c), and the result of traveltimes modelling is shown in dashed line (c) in Figure 5, which has 0.5–2.5 s later than the Pw2 phase.

(4) Multiples inside sedimentary cover: we postulate that the Pw1 and Pw2 phases are multiples that successively reflected by the crystalline basement, the surface, the Moho or LAB interface, respectively (Figure 4d). The results obtained from the forward modelling are shown in dashed line (d) in Figure 5, the theoretical and observed travel times fitted well.

To investigate the reliability of these results, a qualitative comparison of the record section with synthetic seismogram (Figure 6c) calculated using the TRAMP code of Zelt and Forsyth (1994). Furthermore, detailed forward modelling of all refracted and reflected phases identified was undertaken using raytracing method. The observed and calculated traveltimes are shown in Figure 6b. Figure 6a shows the distribution of ray, and the normalized misfit values and the RMS traveltime residual are summarized in Table 1 for each phase. In our study, the percentage of picks that were model is greater than 90 percent of the total picked traveltimes, and the final RMS is nearly equal to the average phase uncertainty indicates that the data have not been overfitting.

3.4 Interpretation and discussion

Putting all evidence together, we find the Pw1 phase is multiples which successively reflected by the crystalline basement, the surface, the Moho and then received on the surface, meanwhile, Pw2 phase is multiples that successively reflected by the crystalline basement, the surface, the LAB and finally received on the surface. However, the two phases are only observed on the record section from the eastern branch of the Sp5 shot on all profile, which indicates the complexity of generating multiples. Previous studies show that the shot Sp5 is located in Jizhong depression of the North China rifted basin with the thickness of sedimentary cover about 4.5–5.0 km. It is possible, therefore, that the significant velocity difference (about 0.8–1.0 km/s) between the sedimentary cover and the crystalline crust is the main reason for generating the two multiple phases and the recording section with high signal to noise ratio make it possible to be observed. Furthermore, the Pw1 and Pw2 multiple phases discussed in this paper can provide the secondary constraints on the velocity model, and constitute seismological evidence for the lithospheric thinning in the eastern NCC.

In the past, multiple reflections are often regarded as noise in the seismological field, and various methods are proposed to suppress multiples. Nowadays, with the development of data processing technology, multiples have been used in structure imaging. The multiple migrations result of the South China sea processed by Liu et al. (2015) shows the advantages of multiple migration. Jia et al. (2017) got well constrained crustal structure model of Bayan Har block by fitting the traveltime of primary and secondary reflection waves in the deep seismic sounding profile. Wang et al. (2018) improved the precision of the crustal structure imaging by exploiting the information of the multiples in the OBS records. Therefore, the multiple wave analysis will become an important research branch in the deep seismic sounding field.

4 Conclusions

(1) Two multiple seismic phases Pw1 and Pw2, which

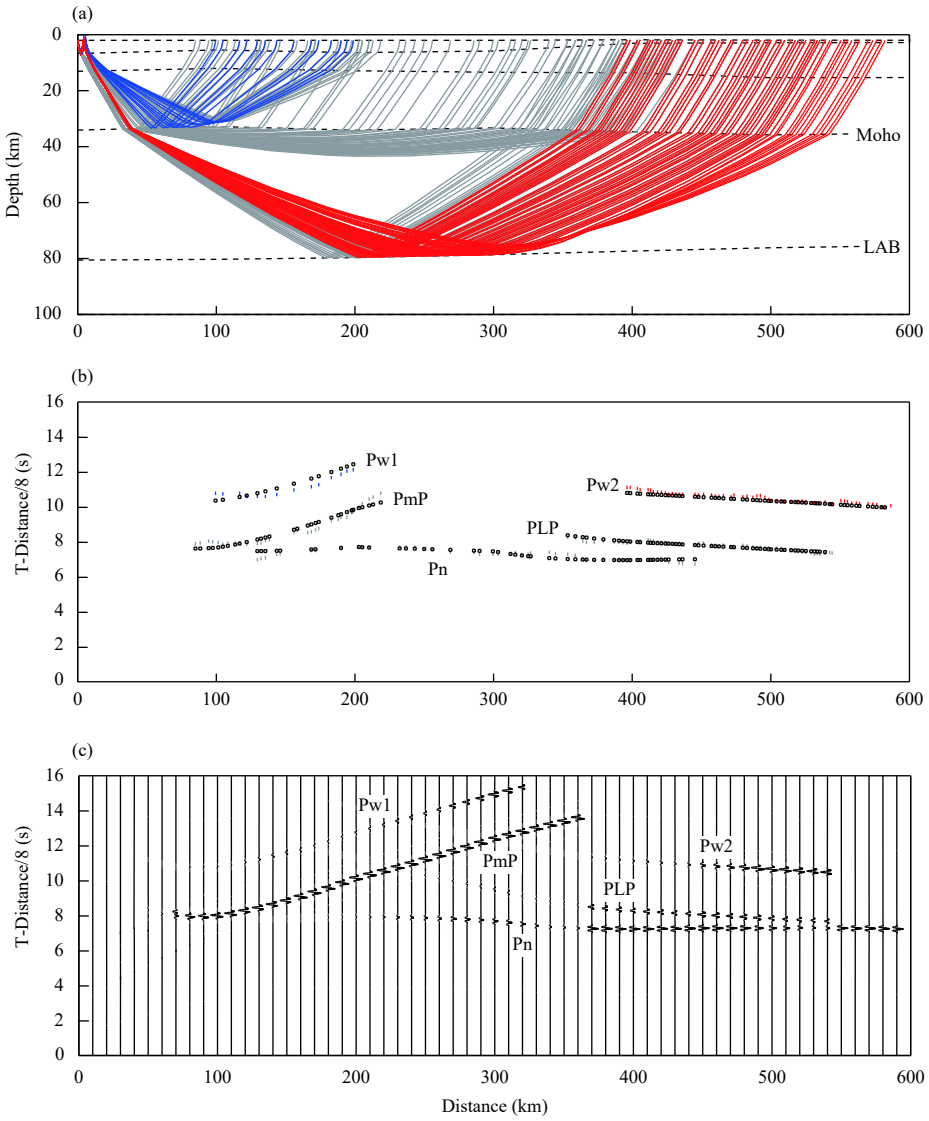

Figure 6 Results of multiples inside crystalline basement. (a) Ray tracing, the blue line indicates the ray trace of Pw1 phase and the red line indicates the ray trace of Pw2 phase; (b) traveltime fitting, the blue dots indicate the calculated traveltimes of Pw1 phase, the red dots indicate the calculated traveltimes of Pw2 phase and the black dots indicate the picked traveltimes of phases; (c) synthetic seismogram

Table 1 Numerical results of traveltime fitting for each phases

Phase type	Traveltime number	Number of ray path	RMS traveltime residual (s)	Chi-square value (s^2)
PmP	31	31	0.275	7.821
Pn	51	51	0.165	2.790
PLP	56	54	0.101	1.031
Pw1	14	14	0.333	11.948
Pw2	60	58	0.151	2.322
All phases	212	208	0.186	3.461

are parallel to deep reflection seismic phases PmP and PLP, respectively, are found on the record section from the east branch of shot Sp5 in the deep sounding seismic profile of NNC. Forward modelling results show that the

two phases are multiple reflection phase which successively reflected by the crystalline basement, the surface and the Moho or the LAB discontinuity.

(2) Two multiple reflected phases may be caused by the thick sedimentary cover and significantly velocity difference between the sedimentary cover and the crystalline crust of the North China rifted basin.

(3) Multiple wave analysis will become an important research branch in the deep seismic sounding field.

Acknowledgements

We gratefully acknowledge the data collection from Geophysical Exploration Center, China Earthquake Administration. This research is financially supported by the National Key Research and Development Program of China (No. 2016YFC0600101), National Natural Science Foundation of China (Nos. 90814012, 41874065 and 41774097) and the Doctor fund of Binzhou University (No. 2018Y15). We appreciate the valuable comments proposed by two anonymous reviewers.

References

Chang X, Liu Y, Zhai M and Wang Y (2007) Crustal P-wave velocity distribution and metallotectonics around the North China, in Mesozoic Sub-Continental Lithospheric Thinning Under Eastern Asia. Geological Society London Special Publications **280**: 293–302

Chen L, Wang T, Zhao L and Zheng TY (2008) Distinct lateral variation of lithospheric thickness in the Northeastern North China Craton. Earth Planet Sci Lett **267**: 56–68

Chen L, Cheng C and Wei ZG (2009) Seismic evidence for significant lateral variations in lithospheric thickness beneath the central and western North China Craton. Earth Planet Sci Lett **286**: 171–183

Chen L (2010) Concordant structural variations from the surface to the base of the upper mantle in the North China Craton and its tectonic implications. Lithos **120**: 96–115

Chen L, Jiang MM, Yang JH, Wei ZG, Liu CZ and Ling Y (2014) Presence of an intralithospheric discontinuity in the central and western North China Craton: Implications for destruction of the craton. Geology **42**(3): 223–226

Duan YH, Liu BJ, Zhao JR, Liu BF, Zhang CK, Pan SZ, Lin JY and Guo WB (2015) 2-D P-wave velocity structure of lithosphere in the North China tectonic zone: Constraints from the Yancheng-Baotou deep seismic profile. Sci China Earth Sci **58**: 1577–1591

Duan YH, Wang FY, Zhang XK, Lin JY, Liu Z, Liu BF, Yang ZX, Guo WB and Wei YH (2016) Three dimensional crustal velocity structure model of the middle-eastern North China Craton (HBCrust1.0). Sci China Earth Sci **59**: 1477–1488

Egorkin AV (1998) Velocity structure, composition and discrimination of crustal provinces in the former Soviet Union. Tectonophysics **298**(4): 395–404

Jia SX, Lin JY, Guo WB, Zhao N and Qiu Y (2017) Investigation on diversity of crustal structures beneath the Bayan Har block. Chin J Geophys **60**(6): 2226–2238 (in Chinese with English abstract)

Jia SX, Wang FY, Tian XF, Duan YH, Zhang JS, Liu BF and Lin JY (2014) Crustal structure and tectonic study of North China Craton from a long deep seismic sounding profile. Tectonophysics **627**: 48–56

Jia SX, Zhang CK, Zhao JR, Fang SM, Liu Z and Zhao JM (2009) Crustal structure of the rift-depression basin and Yanshan uplift in the northeast part of North China. Chin J Geophys **52**(1): 99–110 (in Chinese with English abstract)

Lin G, Wang Y, Guo F, Wang YJ and Fan W (2004) Geodynamic modelling of crustal deformation of the North China block: a preliminary study. Journal of Geophysics and Engineering **1**: 63–69

Liu DY, Nutman AP, Compston W, Wu JS and Shen QH (1992) Remnants of ≥3800 Ma crust in the Chinese part of the Sino-Korean Craton. Geology **20**: 339–342

Liu YK, Zhu WL, Mi LJ, Zhou JX and Hao H (2015) Migration of multiples from the South China Sea. Sci China Earth Sci **58**: 482–490

Liu Z, Wang FY, Zhang XK, Duan YH, Yang ZX and Lin JY (2015) Seismic structure of the lithosphere beneath Eastern North China craton: results from long distance deep seismic sounding. Chin J Geophys **58**(4): 1145–1157 (in Chinese with English abstract)

Malinowski M, Sroda P, Grad M and Guterch A (2009) Testing robust inversion strategies for three-dimensional Moho topography based on CELEBRATION 2000 data. Geophys J Int **179**(2): 1093–1104

Prodehl C and Mooney WD (2012) Exploring the Earth's crust: history and results of controlled-source seismology. Geological Society of America Memoir 208, pp764. doi: 10.1130/2012.2208

Roller JC and Jackson WH (1966) Seismic wave propagation in the upper mantle: Lake Superior, Wisconsin, to central Arizona. J Geophys Res **71**(24): 5933–5941

Rudnick RL and Fountain DM (1995) Nature and composition of the continental crust: a lower crustal perspective. Rev Geophys **33**: 267–309

Teng JW, Zhang ZJ, Zhang XK, Wang CY, Gao R, Yang BJ, Qiao YH and Deng YF (2013) Investigation of the Moho discontinuity beneath the Chinese mainland using deep seismic sounding profiles. Tectonophysics **609**: 202–216

Tian XF, Zelt CA, Wang FY, Jia SX and Liu QX (2014) Crust structure of the North China Craton from a long-range seismic wide-angle-reflection/refraction data. Tectonophysics **634**: 237–245

Wang AX, Wei XD, Ruan AG, Hu H, Wang W, Niu XW and Zhang J (2018) The identification and application of multiple phases recorded by ocean bottom seismometer. Chin Sci Bull **63**: 1235–1244

Wang SJ, Wang FY, Zhang JS, Jia SX, Zhang CK, Zhao JR and Liu BF (2014) The P-wave velocity structure of the lithosphere of the North China Craton-Results from the Wendeng-Alxa Left Banner

deep seismic sounding profile. Sci China Earth Sci **57**: 2053–2063

Wang Y, Houseman GA, Lin G, Guo F, Wang YJ, Fan WM and Chang X (2005) Mesozoic lithospheric deformation in the North China block: numerical simulation of evolution from orogenic belt to extensional basin system. Tectonophysics **405**(1-4): 47–63

Wu FY, Lin JQ, Wilde SA, Zhang XO and Yang JH (2005) Nature and significance of the Early Cretaceous giant igneous event in eastern China. Earth Planet Sci Lett **233**: 103–119

Xu T, Xu GM, Gao EG, Li YC, Jiang XY and Luo KY (2006) Block modeling and segmentally iterative ray tracing in complex 3D media. Geophysics **71**: T41–T51

Xu T, Zhang ZJ, Gao EG, Xu GM and Sun L (2010) Segmentally Iterative Ray Tracing in Complex 2D and 3D Heterogeneous Block Models. Bull Seismol Soc Amer **100**(2): 841–850

Xu T, Li F, Wu ZB, Wu CL, Gao EG, Zhou B, Zhang ZJ and Xu GM (2014) A successive three-point perturbation method for fast ray tracing in complex 2D and 3D geological models. Tectonophysics **627**: 72–81

Xu T, Zhang ZJ, Liu BF, Chen Y, Zhang MH, Tian XB, Xu YG and Teng JW (2015) Crustal velocity structure in the Emeishan large igneous province and evidence of the Permian mantle plume activity. Sci China Earth Sci **58**: 1133–1147

Xu T, Zhang ZJ, Tian XB, Liu BF, Bai ZM, Lü QT and Teng JW (2014b) Crustal structure beneath the Middle-Lower Yangtze metallogenic belt and its surrounding areas: Constraints from active source seismic experiment along the Lixin to Yixing profile in East China. Acta Petrologica Sinica **30**(4): 918–930 (in Chinese with English abstract)

Xu T, Zhang MH, Tian XB, Zheng Y, Bai ZM, Wu CL, Zhang ZJ and Teng JW (2014a) Upper crustal velocity of Lijiang-Qingzhen profile and its relationship with the seismogenic environment of the M_S6.5 Ludian earthquake. Chin J Geophys **57**(9): 3069–3079 (in Chinese with English abstract)

Xu YG (2001) Thermo-tectonic destruction of the Archean lithospheric keel beneath the Sino-Korean Craton in China: Evidence, Timing and Mechanism. Phys Chem Earth Solid Earth Geodes **26**(9-10): 747–757

Xu YG (2004b) Early Cretaceous gabbroic complex from Yinan, Shandong Province: petrogenesis and mantle domains beneath the North China Craton. Int J Earth Sci **93**(6): 1025–1041

Zelt CA and Smith RB (1992) Seimic traveltime inversion for 2-D crustal velocity structure. Geophys J Int **108**: 16–34

Zelt CA and Forsyth DA (1994) Modelling of wide-angle seismic data for crustal structure: Southeastern Grenville Province. J Geophys Res **99**(B6): 11687–11704

Zhang H (2005) Transformation of lithospheric mantle through peridotite-melt reaction: A case of Sino-Korean Craton. Earth Planet Sci Lett **237**: 768–780

Zhang MH, Xu T, Lü QT, Bai ZM, Wu CL, Wu ZB and Teng JW (2015) 3D Moho depth beneath the middle-lower Yangtze metallogenic belt and its surrounding areas: Insight from the wide angle seismic data. Chin J Geophys **58**(12): 4360–4372 (in Chinese with English abstract)

Zhang ZJ, Chen QF, Bai ZM, Chen Y and Badal J (2011) Crustal structure and extensional deformation of thinned lithosphere in Northern China. Tectonophysics **508**: 62–72

Zhang ZJ, Gao R, Bai ZM and Wang HY (2013) Seismological research methods of the crustal fine structure. In Ding ZL, ed. Research Methods of Solid Earth Science. Beijing, Science Press, pp352−368

Zhao GC, Sun M, Wilde SA and Li SZ (2005) Late Archean to Paleoproterozoic evolution of the North China Craton: Key issues revisited. Precambrian Research **136**: 177–202

Zhao GC, Wilde SA, Cawood PA and Sun M (2001) Archean blocks and their boundaries in the North China Craton: Lithological, geochemical, structure and P-T path costraints and tectonic evolution. Precambrian Research **107**(1-2): 45–73

Zhao L, Allen RM, Zheng TY and Hung SH (2009) Reactivation of an Archean craton: Constraints from P- and S-wave tomography in North China. Geophys Res Lett **36**: L17306

Zhao JR, Zhang XK, Wang FY, Zhang CK, Zhang JS, Lin BF and Pan SZ (2009) North China sub-craton lithospheric structure elucidated through coal mine blasting. Chin Sci Bull **54**(4): 669–676 (in Chinese with English abstract)

Zhao L, Allen RM, Zheng TY and Zhu RX (2012) High-resolution body-wave tomography models of the upper mantle beneath eastern China and the adjacent areas. Geochem Geophys Geosyst **13**: Q06007

Zheng TY, Duan YH, Xu WW and Ai YS (2017) A seismic model for crustal structure in North China Craton. Earth and Planetray Physics **1**: 26–34

Zheng TY, Zhao L and Chen L (2005) A detailed receiver function image of the sedimentary structure in the Bohai Bay Basin. Phys Earth Planet Inter **152**: 129–143

Zheng TY, Zhao L, Xu WW and Zhu RX (2008) Insight into modification of North China Craton from seismological study in the Shandong Province. Geophys Res Lett **35**: L22305

Zheng TY, Zhao L and Zhu RX (2009) New evidence from seismic imaging for subduction during assembly of the North China Craton. Geology **37**: 395–398

Zheng TY, Zhao L, He YM and Zhu RX (2014) Seismic imaging of crustal reworking and lithospheric modification in eastern China. Geophys J Int **196**: 656–670

Zheng TY, He YM, Yang JH and Zhao L (2015) Seismological constraints on the crustal structures generated by continental rejuvenation in northeastern China. Scientific Reports **5**: 14995

Zhu RX, Chen L, Wu FY and Liu ZL (2011) Timing, scale and mechanism of the destruction of the North China Craton. Sci China Earth Sci **54**: 789–797

Zhu RX, Xu YG, Zhu G, Zhang HF, Xia QK and Zheng TY (2012) Destruction of the North China Craton. Sci China Earth Sci **55**: 1565–1587

Zhu RX, Zhang HF, Zhu G, Meng QR, Fan HR and Yang JH (2017) Craton destruction and related resoureces. Int J Earth Sci-Geol Rundsch **106**: 2233–2257

Zhu RX and Zheng TY (2009) Destruction geodynamics of the North China Craton and its Paleoproterozoic plate tectonics. Chin Sci Bull **54**: 3354